Available online at www.sciencedirect.com

ScienceDirect

Energy Procedia 99 (2016) 72 – 79

Energy Procedia

10th International Renewable Energy Storage Conference, IRES 2016, 15-17 March 2016, Düsseldorf, Germany

Granular Flow Field In Moving Bed Heat Exchangers: A Continuous Model Approach

Philipp Bartsch[a,*], Torsten Baumann[b], Stefan Zunft[a*]

[a]*Institute of Engineering Thermodynamics, German Aerospace Center, Pfaffenwaldring 38-40, D-70569 Stuttgart, Germany*
[b]*Institute of Solar Research, German Aerospace Center, Karl-Heinz-Beckurts-Str. 13, Jülich, Germany*

Abstract

Moving Bed Heat Exchangers (MBHX) are a promising option to discharge thermal energy from hot bulk materials, which can be used in solar thermal power plants as heat transfer and storage medium. A precise determination of the flow field in a MBHX is required to predict its thermal performance. This paper presents a continuous model approach, based on the theory of soil mechanics to describe the granular flow inside the heat exchanger. The simulation results are compared to a preceding model and experimental data. For this purpose two different tube bundle geometries are analyzed. The results are evaluated by means of contour plots of the flow field and the velocity magnitude of the granular material at the tube surfaces. The new model captures the flow at the top of the tubes quite well but shows need for further improvement in the lower part of the tubes.

Peer-review under responsibility of EUROSOLAR - The European Association for Renewable Energy

Keywords: moving bed, granular flow, thermal energy storage, heat exchanger, renewable energies, concentrating solar power plants;

1. Introduction

In concentrating solar power (CSP) plants, the electric power generation can be decoupled from the instantaneous solar irradiation by using a thermal energy storage (TES) system. This increases the flexibility of the power plant.

* M.Sc. Philipp Bartsch. Tel.: +49-711-6863-753; fax: +49-711-6863-747.
E-mail address: Philipp.bartsch@dlr.de

Peer-review under responsibility of EUROSOLAR - The European Association for Renewable Energy
doi:10.1016/j.egypro.2016.10.099

The suitability of a TES system mainly depends on the heat storage material being used. One possible option are molten salts and their mixtures. However, typical limitations of these materials are the limited temperature range, the technical effort to avoid solidification, the corrosion behavior and the relatively high costs [1].

As opposed to this, fine grained materials are thermally stable at temperatures above 1000 °C. Furthermore, they are environmentally friendly and can be very cost efficient, especially when using natural stones like quartz sand. Therefore, these materials are considered for CSP plants (e.g. [2, 3]). The idea is to heat up the material (> 800 °C) by concentrated solar radiation and store the hot material inside a thermally isolated tank. According to the requirements, hot material can be discharged from the tank to generate steam in a Rankin Cycle and to produce electricity.

One of the key questions regarding this concept is how to discharge thermal energy from the hot granular material. For this purpose a moving bed heat exchanger (MBHX) is suitable due to low parasitic loads and a good performance when operated at part load [2]. Inside this component, the granular material moves slowly downwards, driven by gravity, flowing around heat exchanging surfaces, e.g. tubes which are traversing the bulk material (Fig 1).

The efficient construction of such a MBHX requires a detailed prediction of the heat transferring properties. Unfortunately, granular materials show a different flowing behavior than Newtonian fluids. One of the main differences is that they can form stagnant areas, where the flow completely comes to rest (see Fig. 1, left). This is of particular interest in the vicinity of the tubes, where the resting particles may lead to a strong reduction of heat transfer at the tube surface. Therefore it is of great importance to correctly predict the flow field around the tubes in order to correctly predict the thermal performance of the device.

In preceding works [4, 5] bulk flow in a MBHX has already been modeled by describing the granular material as a continuous medium. However, the approaches were either very simple or could not properly capture the formation of the stagnating zones mentioned above.

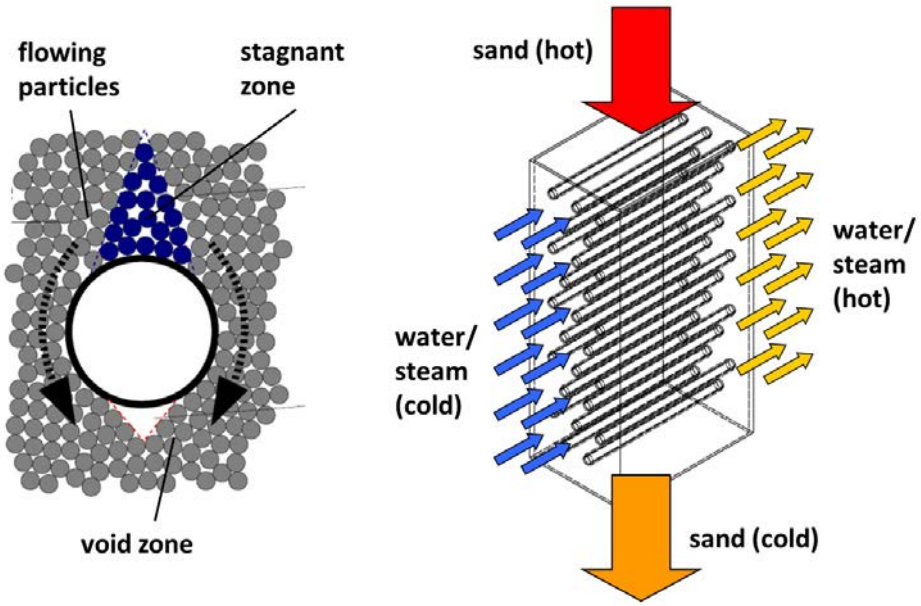

Fig. 1. Flow field around tube (left) and schematic sketch of a moving bed heat exchanger (right).

The model used in this work follows the approach of Baumann et al. [4, 2], by making use of the Eulerian multiphase flow model. This approach treats the bulk as two continuous phases interpenetrating each other. One

phase represents the solid material, the other one the gas (air) filling the voids between the solid particles. Compared to the model of Baumann, in this work the description of the granular phase has been modified.

The behavior of slow, dense granular flows has been modeled in the past using concepts from soil mechanics [6]. The main idea is that the material begins to flow when a certain yield point is reached. In this work such an approach is utilized to model the granular flow inside a MBHX.

2. Methodology

Modelling of granular media here mainly means the modelling of the mechanical interaction between grains inside the granular assembly. In the continuous model these interactions are described as stresses. In rapid and dilute granular flows grains primarily interact through binary collisions, e.g. in fluidized beds. This case has successfully been modelled using the kinetic theory of granular gases (KTGF)[7] which can be seen analogously to the kinetic theory of gases.

2.1. Frictional stress model

By contrast, in dense and slow granular flows like in a moving bed particles mainly interact through frictional contacts with multiple neighbors [8]. This case is subject to soil mechanics, describing the relation between (frictional) stresses and plastic deformations of the bulk. Typically a Newtonian form of the stress tensor is used to express this relation [9]:

$$\boldsymbol{\sigma}_\mathrm{f} = p_\mathrm{f}\mathbf{I} + \eta_\mathrm{f}\mathbf{D} \tag{1}$$

Where **D** is the strain rate or rate of deformation tensor

$$\mathbf{D} = \frac{1}{2}(\nabla\mathbf{v} + (\nabla\mathbf{v})^T) \tag{2}$$

p_f and η_f are called frictional pressure and frictional viscosity, respectively, and have to be defined by constitutive relations. The frictional pressure represents the repulsive forces between grains and prevents the bulk from being compressed beyond a maximum packing limit $\varepsilon_{s,max}$, i.e. the pressure diverges when $\varepsilon_{s,max}$ is approached. For the frictional pressure, a formulation of Johnson and Jackson [10] is used:

$$p_\mathrm{f} = Fr\frac{(\varepsilon_\mathrm{s} - \varepsilon_\mathrm{s,min})^n}{(\varepsilon_\mathrm{s,max} - \varepsilon_\mathrm{s})^p} \tag{3}$$

Here, $\varepsilon_\mathrm{s,min}$ denotes the loosest packing, where frictional interactions occur between the grains. For $\varepsilon_\mathrm{s} < \varepsilon_\mathrm{s,min}$ the frictional pressure is set to zero. This case, though, is not relevant in a moving bed. The parameters in eq. (3) are chosen according to Johnson and Jackson [10] and are listed in Tab. 1.

The frictional viscosity η_f is modelled according to Pitman and Schaeffer [6] in a compressive sense:

$$\eta_\mathrm{f} = \frac{\tau_\mathrm{yield}}{\sqrt{2}\cdot|\mathbf{S}|} \tag{4}$$

$|\mathbf{S}|$ denotes the norm of the deviatoric part of the strain rate **D**. τ_yield is the yield criterion denoting the shear stress at which the material starts to flow. For the yield stress a simple coulomb yield condition is chosen

$$\tau_{\mathrm{yeld}} = \mu_{\mathrm{i}} \cdot p_{\mathrm{f}} \tag{5}$$

with the inner friction coefficient μ_{i}. The coefficient of internal friction is usually set to a constant value which only depends on the inner friction angle [11]. In contrast to that, da Cruz et al. [12] observed variations of the effective friction coefficient and proposed a formulation which depends on material parameters as well as on a dimensionless number I_{s}.

$$\mu_{\mathrm{i}}(I_s) = \mu_{st} + \frac{\mu_{\mathrm{c}} - \mu_{\mathrm{st}}}{I_0 / I_s + 1} \tag{6}$$

I_{s} is called the inertial number and is defined as follows:

$$I_{\mathrm{s}} = \frac{\mathbf{S} \cdot d_{\mathrm{s}}}{\sqrt{p_{\mathrm{f}} / \rho_s}} \tag{7}$$

The inertial number is used as a measure for the state of flow of the bulk material, which can be divided into a quasi-static, an intermediate and a collisional regime [12]. The parameters in eq. (3) and eq. (6) are given in Tab. 1**.**

Eq. (3) includes the assumption that the granular flow takes place under conditions very close to the critical state which means that the effect of dilatancy inside the material is not taken into account. This has been proven as a reasonable assumption for flows in hoppers [11] and for particles being discharged from a bin [8]. Therefore, in this case the assumption is also used in order to stick to a relatively simple model.

2.2. Wall shear stress boundary condition

At a solid wall it must be decided whether the granular material slips along the wall or whether it sticks to the wall. In other words it must be distinguished between sliding and non-sliding contacts. This is of particular importance to predict the heat transfer at the surface.

The distinction between the two cases is achieved by first calculating the shear stress in the slip case according to the Coulomb friction law

$$\tau_{\mathrm{w,sl}} = p_{\mathrm{f}} \cdot \mu_{\mathrm{w}}, \tag{8}$$

with μ_{w} being the coefficient of friction between wall and granular material which has been determined from measurements. The value $\tau_{\mathrm{w,sl}}$ is compared to the viscous shear stress $\tau_{\mathrm{w,ns}}$ in the vicinity of the wall assuming no-slip at the wall. The smaller value of $\tau_{\mathrm{w,sl}}$ and $\tau_{\mathrm{w,ns}}$ is chosen as the shear stress at the wall. This approach has also been used by Schneiderbauer et al. [13], who modelled the discharge of granular material from a bin. For the gas-phase, no-slip boundary conditions are used at walls.

2.3. Coupling between granular an gaseous phase

The coupling terms are chosen the same as in the work of Baumann [4]. The thermal coupling is modelled by a Nusselt correlation of Gunn [14] accounting for the heat transfer between both phases. For the mechanical coupling (Drag) a correlation by Gidaspow [15] is used.

3. Results and discussion

To validate the model the granular flow through two different tube bundle geometries is being simulated (see Fig. 2). In order to compare the results to the model of Baumann, the geometries are chosen the same like in [4]. The material properties and simulation parameters can be found in Tab. 1.

The results presented in the following include contour plots of the velocity field around the tubes and the velocity of the granular phase at the tube surface. Each result is being compared to the corresponding data of Baumann et al. which includes experimental and simulation data. Subsequently the model of Baumann will be referred to as "Model B" and the model introduced in this work will be referred to as "Model A".

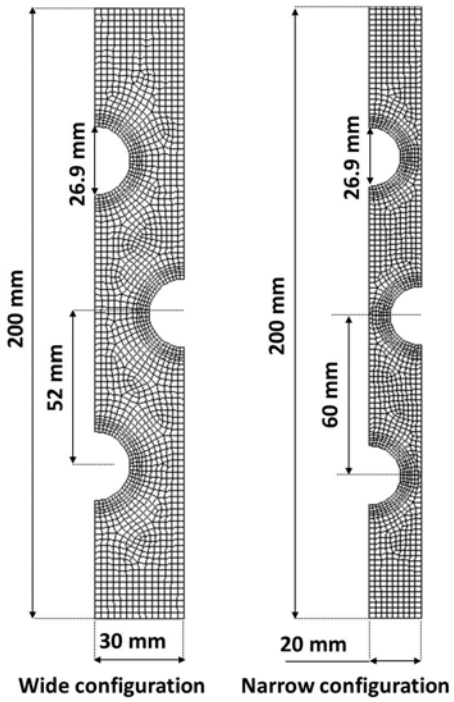

Fig. 2: Investigated tube bundle geometries.

Tab. 1: Values of simulation parameters.

loosest packing (see eq. (3))	ε_{min}	0.5	
densest packing (see eq. (3))	ε_{max}	0.6	
exponent eq. (3)	n	2	
exponent eq. (3)	p	5	
coefficient eq. (3)	Fr	$0.1\varepsilon_s$	
particle diameter	d_p	0.5	mm
wall friction coefficient	μ_w	0.33	
density solid	ρ_s	3900	kg/m³
coefficient eq. (6)	μ_{st}	0,38	
coefficient eq. (6)	μ_c	0,64	
coefficient eq. (6)	I_0	0,279	

3.1. Velocity field

In a first step a qualitative comparison between the flow fields predicted by the two models is drawn. Fig. 3 shows contour plots of the velocity magnitude of the granular phase around the tubes for both geometries compared to measurement data from Baumann. Pictures (a_1) and (a_2) show streamlines of the flow field from time averaged data from PIV measurements. At the top of the tubes the material forms cone shaped stagnant zones bounded by gliding planes with a mean slope angle Θ_{GE} and a mean contact angle Θ_R at the tube surface (see detailed data in [4]).

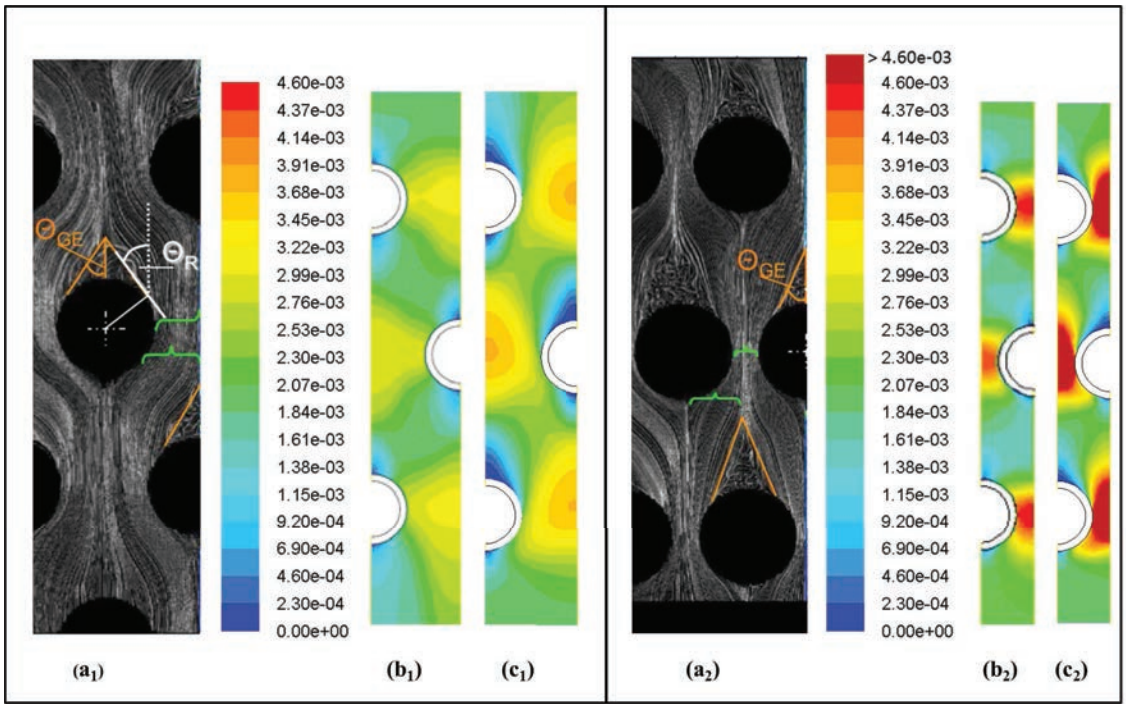

Fig. 3: Flow field around tubes in narrow (subscript "2") and wide (subscript "1") geometry. Streamlines from filtered PIV-measurements for both geometries (a_1, a_2) [4]. Contour plots of velocity magnitude of the granular phase simulated with Model B (b_1, b_2) and Model A (c_1, c_2).

Looking at the simulation results for the wide configuration (see Fig. 2), Model B (b_1) only roughly approximates the true solution for the stagnant zones: It predicts a fuzzy bounded area of reduced flow speed at the top of the tubes. Also, the contour plot shows only small gradients in radial direction at the side of the tubes. The maximum flow speed between the tubes is relatively low. In contrast to that, Model A (c_1) captures the stagnant zones much better. Their size is well predicted, albeit with less sharp boundaries than the measurement data. Also, the slope angle is quite well represented. The deceleration of the granular flow due to wall friction is well reproduced: A distinct gradient of velocity develops in radial direction.

Regarding the narrow configuration, Model B (b_2) yields a similar parabolic profile as for the wide configuration except that the flow speed at the side of the tube is higher. Model A (c_2) also shows higher velocities because of the smaller horizontal cross-section between the tubes. A velocity gradient in radial direction is not visible in the plot because the colored scale is cut off for values > 4.6e-3 m/s, which was necessary to adopt the scale from [4] for reasons of comparability**.** The static zones at the tube vertices are much smaller than in the measurements and the transition from the static to the flowing area is very indistinct.

Altogether, in the narrow configuration the differences between simulation and experiment are more pronounced than in the wide geometry. At this point it has also to be mentioned that for both geometries the void zone below the tubes (see Fig. 1) cannot be reproduced by the model.

3.2. Velocity at tube surface

Having examined the flow field around the tubes in a qualitative way, in this section, quantitative results are shown. For this purpose the velocity of the granular phase at the tube surface is considered. Fig. 4 shows the velocity magnitude of the granular phase along the circumference of a tube for both geometries. A value of y = 0 on the vertical axis corresponds to the bottom of the tube, y = 1 corresponds to the top of the tube (see inlet in Fig. 4).

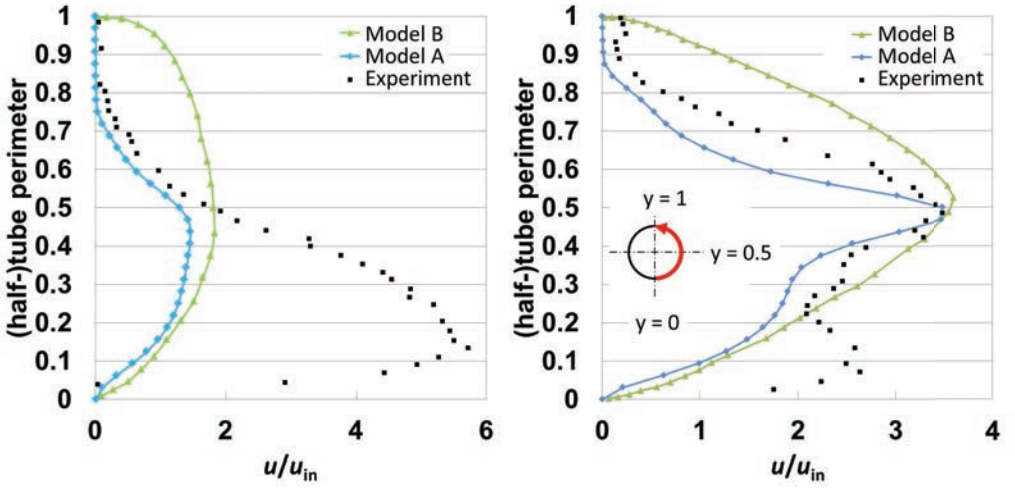

Fig. 4: Velocity magnitude of granular phase at tube surface for the narrow configuration (right) and the wide configuration (left). Experimental data from [4].

For the narrow configuration (on the right in Fig. 4) the experimental data show a stagnant zone at the tube vertex followed by a steep increase of flow speed, reaching a maximum at the side of the tube. In the lower half of the tube, the flow speed does not decrease continuously but exhibits a small plateau before it decreases to zero at the bottom of the tube. This effect is ascribed to the impact of the static zone of the downstream tube row.

For the wide configuration (on the left in Fig. 4) the stagnant zone on the top of the tube is more distinct. The maximum velocity is shifted to the lower half of the tube and reaches higher values than in the narrow configuration. Baumann explained this effect by the smaller vertical distance in the wide configuration (see Fig. 2). Because of the smaller vertical distance, the stagnant zones on top of the subsequent tube row reach into the space between the upstream tubes and reduce the free cross section. As a consequence the flow speed increases according to the law of continuity.

Comparing Model A and B for the narrow configuration, both predict a similar maximum velocity magnitude at the side of the tube which is in good accordance with the experiment. However, the shape of the velocity profiles of the two models is rather different. Model B gives a symmetric and parabolic profile. Model A captures the extent of the static area at the tube vertex much better and the impact of the downstream flow field at the bottom half is quite well represented, albeit less pronounced than in the measurements.

For the wide configuration again both models predict a similar magnitude of maximum velocity at the side of the tube. However, for the reasons explained above the experimentally measured velocity is much higher than in the simulation and shifted to the lower half of the tube. This underestimation of the flow speed shows that the impact of the subsequent row of tubes, which originates from the precise shape of the stagnant areas, is not reproduced with sufficient accuracy. The extent of the area where the material sticks to the tube surface is well predicted by Model A whereas Model B shows a parabolic profile.

4. Conclusion

In this work a new model was presented to predict the flow of granular material around different tube bundle geometries. Compared to previous works, the model clearly yields better results and captures several characteristic features of the complex flow field. The representation of the stagnant areas at the tube vertices has clearly been improved. Especially at the tube surface the extent of the static zone is well predicted. However, the precise shape of the stagnating area is still only roughly reproduced and the transition from the resting to the flowing domain is not as

sharp as in the measurements. In the lower half of the tubes the impact of the downstream flow field is basically reflected. However, the effect is less pronounced than in the measurement data, especially, at small vertical pitches.

Despite these inaccuracies the new model is a promising step towards a more realistic estimation of the flow field in a moving bed heat exchanger. This is an essential prerequisite for a more precise prediction of the thermal performance of the heat exchanger. In a next step the suitability of the model regarding the evaluation of the heat transfer of the MBHX will be tested.

References

[1] D. Kearney, U. Herrmann, P. Nava, B. Kelly, R. Mahoney, J. Pacheco, R. Cable, N. Potrovitza, D. Blake, and H. Price, "Assessment of a Molten Salt Heat Transfer Fluid in a Parabolic Trough Solar Field," *J. Sol. Energy Eng.*, vol. 125, no. 2, p. 170, 2003.

[2] T. Baumann, S. Zunft, and R. Tamme, "Moving Bed Heat Exchangers for Use With Heat Storage in Concentrating Solar Plants: A Multiphase Model," *Heat Transf. Eng.*, vol. 35, no. 3, pp. 224–231, 2013.

[3] C. Ho, J. Christian, D. Gill, A. Moya, S. Jeter, S. Abdel-Khalik, D. Sadowski, N. Siegel, H. Al-Ansary, L. Amsbeck, B. Gobereit, and R. Buck, "Technology advancements for next generation falling particle receivers," *Energy Procedia*, vol. 49, pp. 398–407, 2013.

[4] T. Baumann, "Wärmeauskopplung aus heißen Partikelschüttungen zur Dampferzeugung," University of Stuttgart, 2015.

[5] A. Klein, D. Köneke, and P.-M. Weinspach, "Schüttgutbewegung und Wärmetransport im Wanderbett - Teil 2," *Chemie Ing. Tech.*, vol. 69, pp. 1444–1447, 1997.

[6] E. B. Pitman and D. G. Schaeffer, "Stability of time dependent compressible granular flow in two dimensions," *Comm. Pure Appl. Math.*, vol. 40, no. 4, pp. 421–447, 1987.

[7] J. Ding and D. Gidaspow, "A Bubbling Fluidization Model Using Kinetic Theory of Granular Flow," *AIChE J.*, vol. 36, no. 4, pp. 523–538, 1990.

[8] A. Srivastava and S. Sundaresan, "Analysis of a frictional-kinetic model for gas-particle flow," *Powder Technol.*, vol. 129, no. 1–3, pp. 72–85, 2003.

[9] B. G. M. Van Wachem, J. C. Schouten, C. M. Van den Bleek, R. Krishna, and J. L. Sinclair, "Comparative analysis of CFD models of dense gas-solid systems," *AIChE J.*, vol. 47, no. 5, pp. 1035–1051, 2001.

[10] P. C. Johnson, P. Nott, and R. Jackson, "Frictional–collisional equations of motion for participate flows and their application to chutes," *J. Fluid Mech.*, vol. 210, no. -1, p. 501, 1990.

[11] G. I. Tardos, "A fluid mechanistic approach to slow, frictional flow of powders," *Powder Technol.*, vol. 92, pp. 61–74, 1997.

[12] F. Da Cruz, S. Emam, M. Prochnow, J. N. Roux, and F. Chevoir, "Rheophysics of dense granular materials: Discrete simulation of plane shear flows," *Phys. Rev. E - Stat. Nonlinear, Soft Matter Phys.*, vol. 72, no. 2, pp. 1–17, 2005.

[13] S. Schneiderbauer, A. Aigner, and S. Pirker, "A comprehensive frictional-kinetic model for gas-particle flows: Analysis of fluidized and moving bed regimes," *Chem. Eng. Sci.*, vol. 80, pp. 279–292, 2012.

[14] D. J. Gunn, "Transfer of heat or mass to particles in fixed and fluidised beds," *Int. J. Heat Mass Transf.*, vol. 21, pp. 467–476, 1978.

[15] D. Gidaspow, R. Bezburuah, and J. Ding, "Hydrodynamics of Circulating Fluidized Beds: Kinetic Theory Approach," in *7th Fluidization Conference*, 1992, pp. 1–10.